FRINGE 96
First results from ERS tandem INSAR processing on Svalbard

Knut Eldhuset	Forsvarets Forskningsinstitutt (Norwegian Defence Research Establishment) Knut.Eldhuset@ffi.no http://wwwspace.ffi.no
Frank Aanvik	Universitetet i Oslo (University of Oslo)
Kaare Aksnes	Universitetet i Oslo (University of Oslo)
Jostein Amlien	Norsk Polarinstitutt (Norwegian Polar Institute)
Per Helge Andersen	Forsvarets Forskningsinstitutt (Norwegian Defence Research Establishment)
Svein Hauge	Forsvarets Forskningsinstitutt (Norwegian Defence Research Establishment)
Elisabeth Isaksson	Norsk Polarinstitutt (Norwegian Polar Institute)
Terje Wahl	Forsvarets Forskningsinstitutt (Norwegian Defence Research Establishment)
Dan Johan Weydahl	Forsvarets Forskningsinstitutt (Norwegian Defence Research Establishment)

Abstract

This paper describes some results from a work on how INSAR tandem data can be utilized with the EETF SAR processor combined with the GEOSAT orbit determination program. It is demonstrated how an interferogram simulator can be used to detect errors in existing DEM's and how fringes caused by the terrain can be subtracted from the real interferogram. For the first time it has been possible to monitor motion of the lower part of the fast moving glacier Kronebreen with INSAR due to 1 day interval between the two SAR images. A DEM computed from interferograms (INSAR DEM) over Svalbard is assessed using the existing NP DEM. The precise orbit determination makes the fringes follow the coastline very well over parts of the scene, however, uncertainties in the baseline estimation may cause systematic errors in the INSAR DEM over larger areas in the azimuth direction.

Keywords: SAR processing, orbit determination, interferogram, glacier motion, DEM

1. Introduction

FFI, NP and UiO have recently started an ESA announcement of opportunity project for the scientific exploitation of the ERS Tandem Mission (*Eldhuset et. al.*, 1996a). The ERS Tandem Mission gives unique possibility for testing the limitations of multi-pass INSAR and demonstration of possible applications. Svalbard (79 deg. N, 18 deg. E) has been selected by FFI as test area for that purpose and is one of the most northern populated areas in the world. The low atmospheric humidity, mountain terrain, sparse vegetation and active glaciers make this area very interesting for SAR Interferometry. The paper gives examples of interferograms processed at FFI and a brief description of the processing methods is provided. The importance of precise orbit determination in interferometry is demonstrated.

2. Interferogram generation

All processing steps from raw data to interferogram including precise orbit determination were performed at FFI. The different steps are briefly described below.

2.1 Precise orbit determination and baseline estimation

At FFI a high precision orbit determination software has been developed, called GEOSAT (*Andersen*, 1995a) , (*Andersen et. al.* , 1995b) and (*Andersen* , 1995c). It is unique in the sense that it copes with several types of measurements (e.g. VLBI, SLR, GPS, PRARE, DORIS and WVR). The ERS-1 and ERS-2 orbits were computed for the interferometric pair from 27/28 September 1995 on Svalbard. A geodetic VLBI and PRARE station is located in Ny-Aalesund which is within the test area. The GEOSAT orbit determination yielded rms errors between computed and measured ranges of about 6 cm. Both orbits were transformed to an earth-fixed system to allow estimation of the interferometric baseline components, Bx and By. The baseline components were: Bx=139.44 m, By= -9.16 m at the start of the scenes t1=0 and Bx= 147.55 m ,By= -9.28 at t2=t1+17.1 s. This means that the orbits are non-parallell which would introduce dominating phase ramps if not compensated when generating the interferogram.

2.2 SAR processing

A SAR processor developed at FFI, called second-order Extended Exact Transfer Function (EETF2) (*Eldhuset*, 1995a) and (*Eldhuset*, 1996b), was used to process single look complex images. The EETF2 processor is phase preserving. The interferometric offset test with offset 100 pixels in both azimuth and range yields a mean less than 0.001 degrees and standard deviation less than 2.4 degrees. Figure 1 shows an SAR image around the Woodfjorddalen on Svalbard. The valley to the left in the image is very flat and only few meters above the sea level. The highest peak is around 1300 m. Three distinct glaciers move into this valley from the right.


(Size: 377x447,8-bit)

Figure 1: SAR image around the Woodfjorddalen. Size: 18.1 km in azimuth, 26.8 km in range. The azimuth direction is horizontal. ©ESA/FFI.

2.3 Interferogram generation

Prior to interferogram generation the two tandem scenes are registrated on sub-pixel accuracy. The pixel offsets in both azimuth and range are updated for every new block (Size 690 x 1020 pixels) in both directions when the phase difference from the tandem pair is computed. The compensation of the phase caused by non-parallell orbits and slant range variation is updated for each pixel in both range and azimuth to obtain high interferogram quality.This avoids phase discontinuities at the block boundaries. An ellipsoid was used as earth model. Also, the altitude variation of the satellite above the earth was taken into account. Figure 2 shows an interferogram around the Woodfjorddalen which is almost flat up to the end of the upper glacier in the image. The three glaciers seem to have negligible differential motion since the fringes look like ordinary elevation curves.

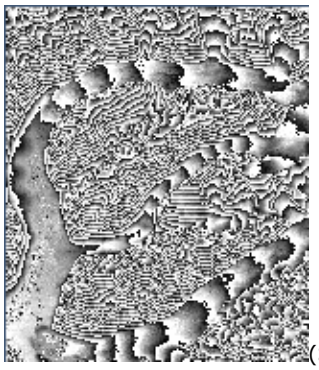 (Size: 377x447,8-bit)

Figure 2: Interferogram around the Woodfjorddalen (same region as in Figure 1). Size: 18.1 km in azimuth, 26.8 km in range. ©ESA/FFI.

2.4 Interferogram simulation

The simulator first performs a registration of the SAR image with the DEM and is nearly identical to the registration part of the FFI ship detector (*Eldhuset*, 1996d) and (*Eldhuset*, 1995b). Then an interferogram simulator computes phase differences using the same two orbits for ERS-1 and ERS-2 as the interferogram generator described in section 2.3. A simulated interferogram covering the same region as in figure 2 is shown in figure 3. It is interesting to note that the river from the upper glacier can be seen in the real interferogram in figure 2, while the simulated interferogram does not show the river. There is a striking similarity between the interferograms in figures 2 and 3.

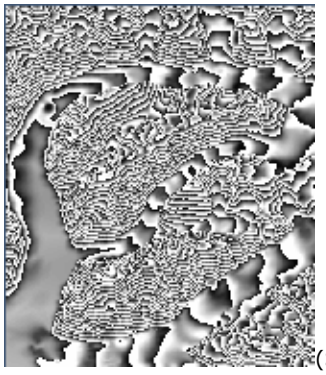 (Size: 377x447,8-bit)

Figure 3: Simulated interferogram around the Woodfjorddalen (same region as in Figure 1). Note that the interferograms in Figures 2 and 3 are not scaled to the same reference phase. Size: 18.1 km in azimuth, 26.8 km in range. ©ESA/NP/FFI.

3. DEM generation

The elevation of ambiguity was estimated using the precise orbits (baseline components) and an ellipsoid as earth model. The elevation of ambiguity was updated for each pixel in the image. The unwrapping was performed using the NP DEM. Over a test region which was 65 km x 42 km , the rms between the NP DEM and the INSAR DEM varied from 12 m to 22 m if the height reference was updated for each processed block. Each processed block was 16.3 km x 14 km. If the height reference was fixed for all of the test region, the rms varied between 15 m to 60 m.

 (Size: 377x447,8-bit)

Figure 4: INSAR DEM around the Woodfjorddalen (same region as in Figure 1). Size: 18.1 km in azimuth, 26.8 km in range. ©ESA/NP/FFI.

4. Assessment of interferogram quality

We now show two methods to assess the interferogram quality. The interferogram can be very easily checked by an investigation of how well the fringes follows the coast line. A more complicated way is to compare an existing DEM with a DEM computed from the real tandem interferogram.

4.1 Assessment of fringe alignment with the shoreline

On Svalbard there are several fiords where it is easy to see whether fringes are parallell with the shoreline. Here we have one example from Dicksonfjorden and Ekmanfjorden (the noisy regions) shown in Figure 5. The GEOSAT program was as mentioned used to compute the ERS-1 and ERS-2 orbits. We see that the fringes follow quite well the shoreline, but not perfectly. When the AO-data have been received and processed we shall investigate the fringes along the 100 km long Widjefjorden.

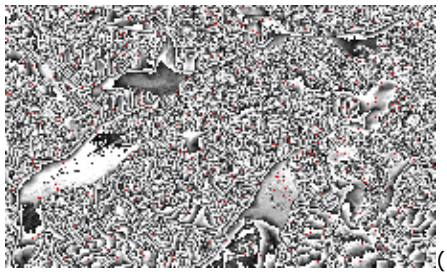 ((Size: 654x404,8-bit)

Figure 5: Interferogram around the Dicksonfjorden and Ekmanfjorden. Size: 41.4 km in azimuth, 32.2 km in range. ©ESA/FFI.

4.2 Comparison of INSAR DEM and existing DEM

When the INSAR DEM was computed we selected a reference height in the existing DEM. We processed blocks of size 690 range x 1020 azimuth pixels. We estimated the mean difference of the heights in the existing NP DEM and the INSAR DEM in each block. An image consisting of 4 azimuth blocks (65 km) and 3 range blocks (42 km) was processed. In figure 6 is shown the mean difference when a block has its own height reference. In figure 7 all blocks have a common height reference. We see that when the height reference is updated for each block, the mean differences oscillate around 0 m. In some cases the difference is very close to 0 m while the worst case is about 22 m. It should be noted that this terrain is rugged with heights from 0 m to 1300 m. In addition some parts of the INSAR DEM has motion fringes where the unwrapping fails. If only one reference heigth was used, there was an obvious drift in the height differences in azimuth direction (see figure 7). The height differences in range direction varied only a few meters. The rms error of 6 cm of the GEOSAT orbits may explain the drift in azimuth direction.

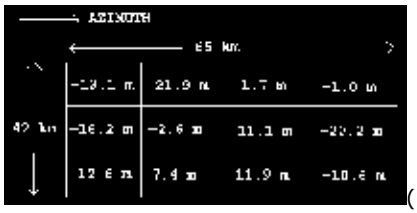
((Size: 496x246,8-bit)

Figure 6: Assessment of INSAR DEM with updated reference ©FFI.

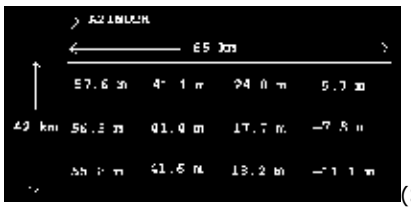
(Size: 496x246,8-bit)

Figure 7: Assessment of INSAR DEM with fixed reference ©FFI.

5. Detection of errors in existing DEM's

It has been demonstarted at FFI that simulation of interferograms from existing DEM's can be used to reveal errors. This can be done by a direct comparison of the real and simulated interferograms. An example in the northern part of Norway can be found in (*Eldhuset*, 1996c). Another example is shown in figures 8 and 9. Figure 8 is real and figure 9 is a simulated interferogram. The interferogram covers part of a glacier with some mountains. Over the mountain areas the interferograms are very similar. An obvious feature in the simulated interferogram is in the middle of the image. This correspond to a hole in the NP DEM. The elevation of ambiguity is around 75 m, so the hole may be 100 m on a rather flat glacier. A corresponding hole is not seen in the real interferogram. In a new version of the DEM at NP the hole is not observed. This version shall be used at FFI in the future.

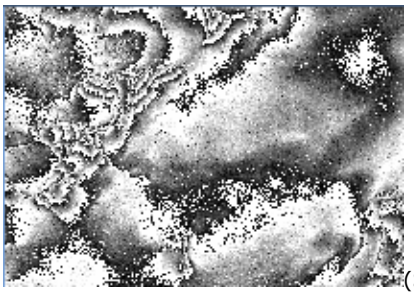 (Size: 543x387,8-bit)

Figure 8: Real interferogram over a glacier with some mountains. Pixel size is 16 m in azimuth and 20 m in ground range. ©ESA/FFI.

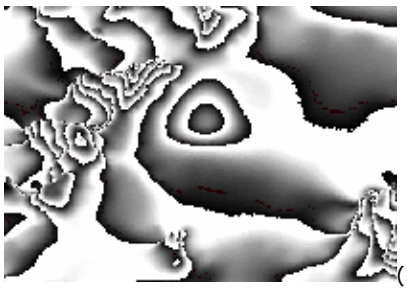 (Size: 543x387,8-bit)

Figure 9: Simulated interferogram over a glacier with some mountains. Pixel size is 16 m in azimuth and 20 m in ground range. ©ESA/NP/FFI.

6. Motion fringes on glaciers

It has already be demonstrated that the ERS-1 can be used to monitor motion of ice sheets with interferometric SAR (INSAR) e.g., see (*Goldstein et. al.* , 1993) and (*Kwock et. al.*, 1996). The ERS-1 had both 3 days and 35 days repeat cycle. The repeat cycle of ERS tandem (ERS-1/ERS-2) is only 1 day and provides the opportunity to monitor faster glaciers than with ERS-1 alone. Tandem data were used in (*Mohr et. al.*, 1996) to study a glacier on Greenland, but they did not have a DEM available.

6.1 Kronebreen and Kongsvegen

Figure 10 shows the SAR image over the two merging glaciers Kronebreen and Kongsvegen. Figure 11 shows an interferogram where fringes caused by slant range variation and non-parallell orbits have been removed using an ellipsoid as earth model. Figure 12 shows the interferogram in Figure 11 when the fringes caused by the terrain have been removed using the NP DEM. It has not been possible to extract motion fringes from ERS-1/ERS-1 interferograms in this part of Kronebreen (*Lefauconnier*, 1996). In our further work we shall monitor the motion fringes throughout the tandem period.

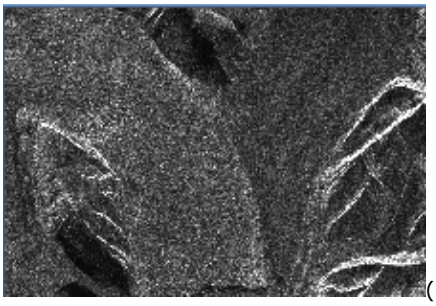 (Size: 636x443,8-bit)

Figure 10: ERS-1 SAR image over Kronebreen (left) and Kongsvegen(right), 27th September 1995. Pixel size is 16 m in azimuth and 20 m in ground range. ©ESA/FFI.

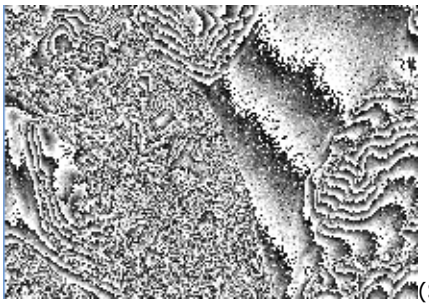 (Size: 636x443,8-bit)

Figure 11: ERS-1/ERS-2 interferogram over the lower parts of the glaciers Kronebreen and Kongsvegen, 27/28 September 1995. ©ESA/FFI.

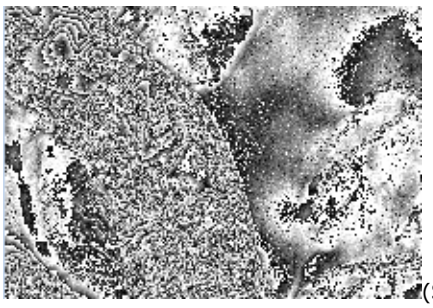 (Size: 636x443,8-bit)

Figure 12: Interferogram in Figure 2 where terrain fringes have been removed using the NP DEM. ©ESA/NP/FFI.

6.2 Preliminary analysis

In figure 11 we can see that even with tandem the interferogram is noisy at the fast moving front of Kronebreen and in the contact zone with Kongsvegen. The most likely explanation for this is probably to be found in the very complicated crevasse pattern, due to high shear stresses, in these parts of the glacier. One can see from Figure 11 that Kronebreen has typical motion fringes while Kongsvegen has mostly terrain fringes. In Figure 12 one can see that when terrain fringes have been subtracted, the remaining fringes on Kongsvegen indicates very small differential motion while on Kronebreen there is a quite complicated motion pattern which is due to differential motion. Field measurements done in 1990 suggests ice velocities of more than 2 m/day in the

central part of Kronebreen while velocities on Kongsvegen are in the order of 1-2 cm/day (*Melvold*, 1992) A photogrammetric study using SPOT images confirmed these velocities for Kronebreen (Lefauconnier et al., 1994). ((*Lefauconnier et al* , 1994)) On both glaciers the ice velocity rapidly decrease towards the margins. The difference in velocity magnitude between these two glaciers is clearly visible in the interferogram. A detailed analysis of the motion pattern is presently being performed at NP. Preliminary results suggests that velocity magnitudes obtained from the interferograms agree with previous studies. It seems like in order to obtain velocity information on glaciers like Kronebreen, where parts of the glacier are heavily crevassed, a combination of field measurements, photogrammetic methods and interferometry are most likely to be successful.

7. Conclusions

We have demonstrated how the EETF SAR processor has been combined with the GEOSAT precise orbit determination software to process a tandem interferogram with high quality. The fringes follows the coast line very good in parts of the scene. An INSAR DEM was generated and compared with an existing DEM. The height differences of the two DEM's are especially dependent of the size of the DEM in azimuth direction if the height reference is fixed. This may be explained by uncertainties in the baseline estimation. It was shown how an interferogram simulator can be used to reveal errors in an existing DEM. For the first time ice velocity on the fast moving glacier Kronebreen has been estimated using SAR interferometry. Velocity magnitudes extracted from the interferogram agree well with ground measurements and estimation from SPOT images.

8. Acknowledgement

The FFI EETF SAR processor has been industrialized by the Norwegian company Kongsberg Informasjonskontroll (KIK) and has been delivered to th National University of Singapore for ERS-1 processing. It is currently installed at Tromsoe Satellite Station for RADARSAT processing. The work described in this paper is partly supported by the Norwegian Space Center.

References

Andersen P.H., 1995a:
High-precision station positioning and satellite orbit determination. *NDRE/PUBLICATION-95/01094*, Norwegian Defence Research Establishment, P.O. Box 25, 2007 Kjeller, Norway.

Andersen P.H., Hauge S., Kristiansen O., 1995b:
Precise ERS-1 orbit calculation. *Bulletin Geodesique*, vol 69, pp. 192-199.

Andersen P.H., 1995c:
http://wwwspace.ffi.no/SpaceWeb/RSGroup/Orbit_analysis.html.

Eldhuset K., 1995a:
FFI EETF Algorithm 2nd Order . *http://wwwspace.ffi.no/SpaceWeb/RSGroup/FFI_EETF_Alg.html* .

Eldhuset K., 1995b:
Automatic Detection . *http://wwwspace.ffi.no/SpaceWeb/RSGroup/Automatic_detection.html* .

Eldhuset K. (P.I.), Aanvik F., Aksnes K., Andersen K., Hauge S., Isaksson E., Wahl T., Weydahl D.J., 1996a:
ERS tandem interferometric SAR studies on Svalbard . *ESA AOT.N301 project* , 1996-1998.

Eldhuset K., 1996b:
Accurate attitude estimation using ERS-1 SAR raw data . *International Journal of Remote Sensing*, vol. 17,no. 14, pp. 2827-2844.

Eldhuset K. and Wahl T., 1996c:
SAR interferometry for detecting errors in old DEM's .
http://wwwspace.ffi.no/SpaceWeb/RSGroup/HIPSAR/HIPSARNews/News96/ErrorsInOldDEMs.html

Eldhuset K., 1996d:
An automatic Ship and Ship Wake Detection System for Spaceborne SAR Images in Coastal Regions. *IEEE Trans. On Geosc. and Remote Sensing*, vol. 34, no. 4, pp. 1010-1019.

Goldstein R.M., Engelhardt H., Kamb B., Frolich R.M., 1993:
Satellite Radar Interferometry for Monitoring Ice Sheet Motion: Application to an Antarctic Ice Stream. *Science* , vol. 262, pp. 1525-1529.

Kwok R., Fahnestock M.A., 1996:
Ice Sheet Motion and Topography from Radar Interferometry. *IEEE Trans. on Geosc. and Remote Sensing*, vol GRS-34, No 1, pp. 189-200.

Lefauconnier B., Hagen J.O., Rudant J.P., 1994:
Flow speed and calving rate of Kronebreen glacier, Svalbard, using SPOT images. *Polar Research*, vol. 13, no. 1, pp. 59-65.

Lefauconnier B., 1996:
Personal communication.

Melvold K., 1992:
Study of glacier motion on Kongsvegen and Kronebreen, Svalbard. *Technical Report*, Department of Geography, University of Oslo.

Mohr J.J., Madsen S.N., 1996:
Application of Interferometry to Studies of Glacier Dynamics. In: *Proc. IGARSS'96 Symp.*, pp. 972-974.